



This is a repository copy of *Exploring the upper size limit for sterically stabilized diblock copolymer nanoparticles prepared by polymerization-induced self-assembly in non-polar media*.

White Rose Research Online URL for this paper:  
<http://eprints.whiterose.ac.uk/160150/>

Version: Published Version

---

**Article:**

Parker, B.R., Derry, M.J., Ning, Y. et al. (1 more author) (2020) Exploring the upper size limit for sterically stabilized diblock copolymer nanoparticles prepared by polymerization-induced self-assembly in non-polar media. *Langmuir*, 36 (14). pp. 3730-3736. ISSN 0743-7463

<https://doi.org/10.1021/acs.langmuir.0c00211>

---

**Reuse**

This article is distributed under the terms of the Creative Commons Attribution (CC BY) licence. This licence allows you to distribute, remix, tweak, and build upon the work, even commercially, as long as you credit the authors for the original work. More information and the full terms of the licence here:  
<https://creativecommons.org/licenses/>

**Takedown**

If you consider content in White Rose Research Online to be in breach of UK law, please notify us by emailing [eprints@whiterose.ac.uk](mailto:eprints@whiterose.ac.uk) including the URL of the record and the reason for the withdrawal request.



[eprints@whiterose.ac.uk](mailto:eprints@whiterose.ac.uk)  
<https://eprints.whiterose.ac.uk/>

## Exploring the Upper Size Limit for Sterically Stabilized Diblock Copolymer Nanoparticles Prepared by Polymerization-Induced Self-Assembly in Non-Polar Media

Bryony R. Parker, Matthew J. Derry,\* Yin Ning, and Steven P. Armes\*



Cite This: *Langmuir* 2020, 36, 3730–3736



Read Online

ACCESS |



Metrics & More



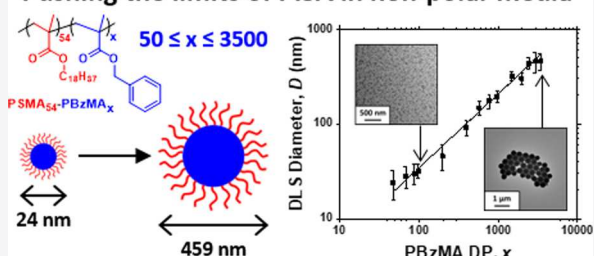
Article Recommendations



Supporting Information

**ABSTRACT:** Reversible addition–fragmentation chain transfer (RAFT) dispersion polymerization of benzyl methacrylate is used to prepare a series of well-defined poly(stearyl methacrylate)–poly(benzyl methacrylate) (PSMA–PBzMA) diblock copolymer nanoparticles in mineral oil at 90 °C. A relatively long PSMA<sub>54</sub> precursor acts as a steric stabilizer block and also ensures that only kinetically trapped spheres are obtained, regardless of the target degree of polymerization (DP) for the core-forming PBzMA block. This polymerization-induced self-assembly (PISA) formulation provides good control over the particle size distribution over a wide size range (24–459 nm diameter). <sup>1</sup>H NMR spectroscopy studies confirm that high monomer conversions (≥96%) are obtained for all PISA syntheses while transmission electron microscopy and dynamic light scattering analyses show well-defined spheres with a power-law relationship between the target PBzMA DP and the mean particle diameter. Gel permeation chromatography studies indicate a gradual loss of control over the molecular weight distribution as higher DPs are targeted, but well-defined morphologies and narrow particle size distributions can be obtained for PBzMA DPs up to 3500, which corresponds to an upper particle size limit of 459 nm. Thus, these are among the largest well-defined spheres with reasonably narrow size distributions (standard deviation ≤20%) produced by any PISA formulation. Such large spheres serve as model sterically stabilized particles for analytical centrifugation studies.

### Pushing the limits of PISA in non-polar media



## INTRODUCTION

Polymerization-induced self-assembly (PISA) has become widely recognized as a powerful platform technology for the rational synthesis of sterically stabilized diblock copolymer nano-objects with various morphologies.<sup>1–5</sup> One of the main advantages of PISA is its versatility: it can be conducted in water,<sup>6–11</sup> polar solvents,<sup>12–19</sup> or non-polar media.<sup>20–29</sup> In essence, PISA involves growing AB diblock copolymer chains in a suitable solvent, i.e. a good solvent for the precursor (A) block but a bad solvent for the growing second (B) block. This scenario leads to *in situ* self-assembly to produce sterically stabilized diblock copolymer nanoparticles whose final copolymer morphology (e.g., spheres, worms/cylinders, or vesicles) should be primarily governed by the relative block volume fractions.<sup>29,30</sup> In practice, using a relatively long A block usually leads to the formation of kinetically trapped spheres.<sup>31</sup> In principle, the design rules for PISA are generic, and various (pseudo)living polymerization chemistries should be applicable. Indeed, there are at least two examples of anionic polymerization being utilized for the formation of diblock copolymer nano-objects.<sup>32,33</sup> However, the vast majority of the PISA literature is based on reversible addition–fragmentation chain transfer (RAFT) polymerization, which offers exceptional tolerance of monomer

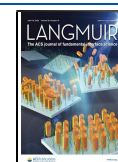
functionality and can be conducted directly in protic solvents.<sup>34–38</sup>

RAFT dispersion polymerization in non-polar media has been reported by various research groups over the past decade. Charleux and co-workers studied the synthesis of poly(2-ethylhexyl acrylate)–poly(methyl acrylate) in isododecane.<sup>20,21</sup> Ratcliffe and co-workers also reported all-acrylic PISA formulations in *n*-heptane, *n*-dodecane or isohexadecane.<sup>39</sup> However, polymerization of methacrylic monomers has generally afforded much better control over the molecular weight distribution and copolymer morphology.<sup>22–29</sup> Thus, Fielding and co-workers reported the PISA synthesis of poly(lauryl methacrylate)–poly(benzyl methacrylate) [PLMA–PBzMA] diblock copolymer spheres, worms or vesicles in *n*-heptane at 90 °C.<sup>29</sup> The same team also demonstrated that PLMA–PBzMA worms prepared in a solvent with a higher boiling point (*n*-dodecane) exhibited a

Received: January 23, 2020

Revised: March 26, 2020

Published: March 26, 2020



reversible worm-to-sphere morphological transition on heating.<sup>22</sup> Similar findings were reported by Lowe and co-workers when using poly(phenylpropyl methacrylate) as the structure-directing block.<sup>25</sup> Derry et al. showed that closely related PISA syntheses yielded well-defined spheres at up to 50% w/w in mineral oil<sup>30</sup> and was subsequently able to monitor the *in situ* evolution in copolymer morphology that occurred when targeting vesicles by small-angle X-ray scattering (SAXS).<sup>26</sup> In this case, poly(stearyl methacrylate) [PSMA] was used as the steric stabilizer block, and higher blocking efficiencies were observed compared to those achieved when using PLMA.

Herein, we revisit the PSMA–PBzMA formulation previously reported by Derry and co-workers.<sup>26,27</sup> We utilize a relatively long PSMA stabilizer block to ensure that the sole copolymer morphology is kinetically trapped spheres and show that systematic variation of the target DP for the core-forming PBzMA block leads to a series of well-defined nanoparticles with reasonably narrow size distributions over a remarkably wide size range. Moreover, there is a strong correlation between the target DP of the PBzMA block and the mean particle diameter, which means that a desired particle size can be readily obtained. Given their ease of synthesis, such sterically stabilized nanoparticles are expected to be used as model systems for fundamental studies in the field of colloid and interface science,<sup>40,41</sup> as well as potential commercial applications.<sup>42–45</sup>

## ■ EXPERIMENTAL SECTION

**Materials.** Benzyl methacrylate (BzMA), 2,2'-azobis(isobutyronitrile) (AIBN), CDCl<sub>3</sub>, and all other reagents were purchased from Sigma-Aldrich and used as received unless otherwise stated. Stearyl methacrylate (SMA) was purchased from Santa Cruz Biotechnology Ltd. 4-Cyano-4-(2-phenylethane sulfanylthiocarbonyl) sulfanylpentanoic acid (PETTC) was synthesized using the protocol reported by Rymaruk et al.<sup>46</sup> *tert*-Butyl peroxy-2-ethylhexanoate (T21s) initiator was purchased from AkzoNobel. Toluene, THF, and *n*-dodecane were purchased from Fisher Scientific, and CD<sub>2</sub>Cl<sub>2</sub> was purchased from Goss Scientific. A 4 cSt American Petroleum Institute (API) Group III mineral oil (2.82% aromatic content) was kindly provided by The Lubrizol Corporation Ltd. (Hazelwood, Derbyshire, UK).

**Synthesis of Poly(stearyl methacrylate) Macromolecular Chain Transfer Agent via RAFT Solution Polymerization.** The synthesis of a PSMA<sub>54</sub> macromolecular chain transfer agent (macro-CTA) at 50% w/w solids was conducted as follows. A 250 mL round-bottomed flask was charged with SMA (29.9 g; 88.2 mmol), PETTC (0.60 g; 1.76 mmol; target degree of polymerization = 50), AIBN (57.9 mg, 0.35 mmol; PETTC/AIBN molar ratio = 5.0), and toluene (30.52 g). The sealed reaction vessel was purged with nitrogen and placed in a preheated oil bath at 70 °C for 4 h. The resulting PSMA (SMA conversion = 78%;  $M_n = 12\,700\text{ g mol}^{-1}$ ,  $M_w = 14\,600\text{ g mol}^{-1}$ ,  $M_w/M_n = 1.15$ ) was purified by precipitation into excess ethanol. The mean degree of polymerization (DP) of this macro-CTA was calculated to be 54 using <sup>1</sup>H NMR spectroscopy by comparing the integrated signals corresponding to the five phenyl end-group protons protons at 7.0–7.5 ppm with that assigned to the two oxymethylene protons of PSMA at 3.8–4.2 ppm.

**Synthesis of Poly(stearyl methacrylate)–Poly(benzyl methacrylate) Diblock Copolymer Spheres via RAFT Dispersion Polymerization.** A typical RAFT dispersion polymerization synthesis of PSMA<sub>54</sub>–PBzMA<sub>1485</sub> diblock copolymer nanoparticles at 20% w/w solids was conducted as follows. BzMA (0.498 g; 2.82 mmol), T21s initiator (0.08 mg; 0.38 μmol; dissolved in 1.0% v/v in mineral oil), and PSMA<sub>54</sub> macro-CTA (0.035 g; 1.88 μmol; macro-CTA/initiator molar ratio = 5.0; target degree of polymerization of PBzMA = 1500) were dissolved in mineral oil (2.13 g). The reaction mixture was sealed in a 10 mL round-bottomed flask and purged with

nitrogen gas for 30 min. The deoxygenated solution was then placed in a preheated oil bath at 90 °C for 5 h (final BzMA conversion = 99%;  $M_n = 111\,400\text{ g mol}^{-1}$ ,  $M_w/M_n = 3.11$ ; nanoparticle diameter =  $320 \pm 32\text{ nm}$ ).

**Gel Permeation Chromatography (GPC).** Molecular weight distributions (MWDs) were assessed by GPC using THF eluent. The THF GPC setup comprised two 5 μm (30 cm) Mixed C columns and a WellChrom K-2301 refractive index detector operating at a wavelength of  $950 \pm 30\text{ nm}$ . The mobile phase contained 2.0% v/v triethylamine and 0.05% w/v butylhydroxytoluene (BHT), and the flow rate was  $1.0\text{ mL min}^{-1}$ . A series of 12 near-monodisperse poly(methyl methacrylate) standards ( $M_p$  values ranging from 654 to  $2\,480\,000\text{ g mol}^{-1}$ ) were used for calibration.

**<sup>1</sup>H NMR Spectroscopy.** <sup>1</sup>H NMR spectra were recorded in either CD<sub>2</sub>Cl<sub>2</sub> or CDCl<sub>3</sub> using a Bruker AV1-400 MHz spectrometer. Typically, 64 scans were averaged per spectrum. Chemical shifts are expressed in ppm and are internally referenced to the residual solvent peak.

**Dynamic Light Scattering (DLS).** DLS studies were performed using a Zetasizer Nano ZS instrument (Malvern Instruments) at a fixed scattering angle of 173°. Copolymer dispersions were diluted in *n*-dodecane (0.10% w/w) prior to light scattering analysis at 25 °C. The intensity-average hydrodynamic diameter ( $D_h$ ) and polydispersity of the diblock copolymer nanoparticles were calculated by cumulants analysis of the experimental correlation function using Dispersion Technology Software version 6.20. Data were averaged over 13 runs each of 30 seconds duration.

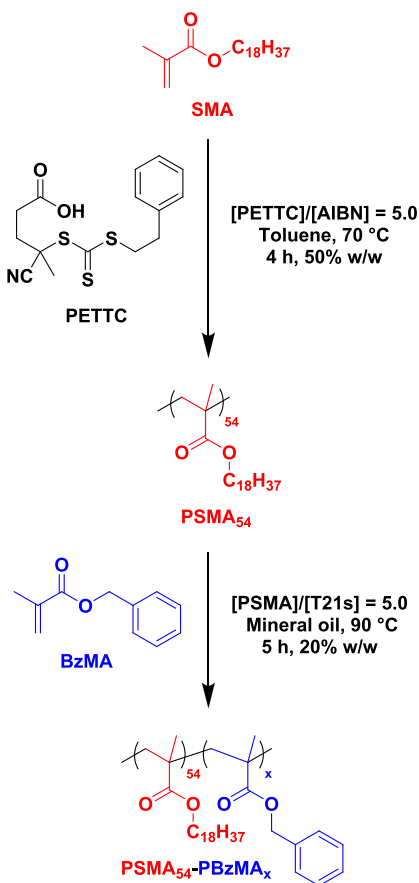
**Transmission Electron Microscopy (TEM).** Transmission electron microscopy (TEM) studies were conducted using a Philips CM 100 instrument operating at 100 kV and equipped with a Gatan 1 k CCD camera. Diluted diblock copolymer solutions (0.10% w/w) were placed as droplets on carbon-coated copper grids, exposed to ruthenium(VIII) oxide vapor for 7 min at 20 °C, and dried prior to analysis.<sup>47</sup> The ruthenium(VIII) oxide solution was prepared as follows: ruthenium(IV) oxide (0.3 g) was added to water (50 g) to form a black slurry; addition of sodium periodate (2.0 g) with stirring produced a yellow solution of ruthenium(VIII) oxide within 1 min. This heavy metal compound acted as a positive stain for the core-forming PBzMA block in order to improve contrast.

**Analytical Centrifugation.** Nanoparticle size distributions were determined using a LUMiSizer analytical photocentrifuge (LUM GmbH, Berlin, Germany) at 20 °C. The LUMiSizer is a micro-processor-controlled instrument that employs space- and time-resolved extinction profiles (STEP) technology for the measurement of the intensity of transmitted light as a function of time and position over the entire cell length simultaneously. The progression of these transmission profiles contains information on the rate of sedimentation and, given knowledge of the effective particle density, enables calculation of the particle size distribution. Measurements were conducted on 1.0% w/w copolymer dispersions at 4000 rpm for 22.22 h (1000 profiles; with 80 s between each profile) using 2 mm path length polyamide cells. Data analysis was conducted assuming a nanoparticle density of  $1.15\text{ g cm}^{-3}$  (i.e., the same density as that of the PBzMA nanoparticle cores alone).

## ■ RESULTS AND DISCUSSION

The main objective of this study was to determine the upper particle size limit that can be accessed using the chosen PISA formulation (see Scheme 1), regardless of the level of RAFT control. The synthesis of larger nanoparticles requires targeting higher degrees of polymerization for the core-forming block. For a given solids concentration, this necessarily means increasing the initial concentration of BzMA monomer relative to that of the steric stabilizer precursor (in this case, the PSMA block). Given that the latter parameter is directly linked to the concentration of the peroxide initiator,<sup>36</sup> this requires a concomitant reduction in the concentration of the latter reagent. Clearly, at some point the initiator concentration will

**Scheme 1. Synthesis of Poly(stearyl methacrylate) (PSMA<sub>54</sub>) Macro-CTA via RAFT Solution Polymerization of Stearyl Methacrylate (SMA) in Toluene Using 4-Cyano-4-(2-phenylethane sulfanylthiocarbonyl) Sulfanylpentanoic Acid (PETTC) at 70 °C, Followed by the RAFT Dispersion Polymerization of Benzyl Methacrylate (BzMA) in Mineral Oil at 90 °C**



become so low that the rate of radical flux is insufficient, leading to either incomplete monomer conversion or no polymerization at all. Thus, an upper particle size limit should be anticipated for all PISA formulations. The question addressed herein is what are the largest well-defined particles of reasonably narrow size distribution that can be accessed for a given formulation, and are such syntheses accompanied by any particular constraints?

Figure 1a shows a series of THF GPC curves recorded for a series of PSMA<sub>54</sub>-PBzMA<sub>x</sub> diblock copolymers. A systematic shift to higher molecular weight is observed when targeting higher PBzMA DPs, and relatively high blocking efficiencies are achieved. More specifically, a linear correlation between  $M_n$  and PBzMA DP is shown in Figure 1b when targeting core-forming block DPs of up to 1000. However, the molecular weight distribution only remains relatively narrow ( $M_w/M_n < 1.25$ ) when targeting PBzMA DPs below 400. Indeed, the  $M_w/M_n$  increases monotonically to 2.50 when targeting PBzMA DPs up to 1000, with values of 2.95–3.41 being obtained for target DPs of 1500–3500 (see Figure 1b and Table 1). Clearly, lower blocking efficiencies are obtained when targeting such high PBzMA DPs, as indicated by the prominent low-molecular-weight shoulder. Similar observations were reported by Derry and co-workers for a closely related PISA

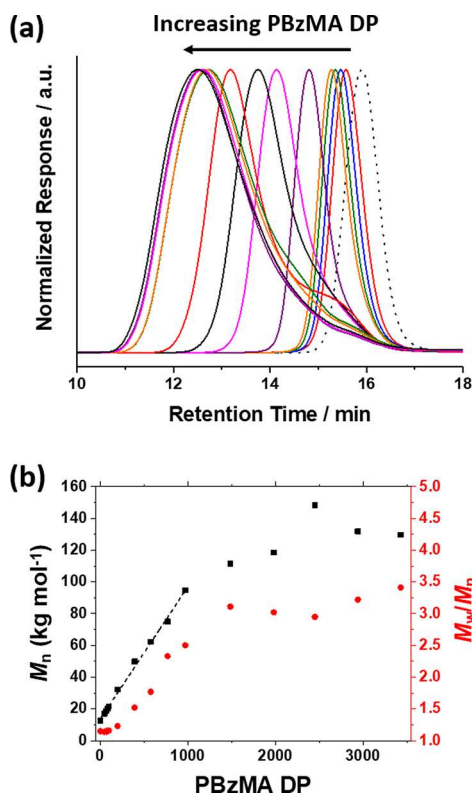


**Figure 1.** (a) THF gel permeation chromatograms (vs poly(methyl methacrylate) calibration standards) obtained for 14 PSMA<sub>54</sub>-PBzMA<sub>x</sub> diblock copolymers prepared via RAFT dispersion polymerization of benzyl methacrylate in mineral oil at 90 °C at 20% w/w solids. The precursor PSMA<sub>54</sub> macro-CTA (prepared in toluene at 70 °C at 50% w/w solids) is also shown as a reference (black dashed curve). (b)  $M_n$  (black ■) and  $M_w/M_n$  (red ●) vs PBzMA DP plots for the series of PSMA<sub>54</sub>-PBzMA<sub>x</sub> diblock copolymers shown in part a. A linear evolution for  $M_n$  vs PBzMA DP is observed for PBzMA DPs  $\leq 1000$ .

formulation.<sup>26</sup> Such broad MWDs clearly indicate a gradual loss of RAFT control during PISA. Moreover, lower blocking efficiencies were observed when targeting higher PBzMA DPs, which suggests relatively slow reinitiation under such conditions.<sup>48,49</sup> Nevertheless, this problem does not prevent the self-assembly of well-defined PSMA<sub>54</sub>-PBzMA<sub>x</sub> particles of reasonably narrow size distribution and predictable particle size over a wide size range (see below). [N.B. Any PBzMA homopolymer chains generated owing to poor RAFT control are expected to be collocated within the nanoparticle cores along with the structure-directing PBzMA blocks.] However, targeting PBzMA blocks with a DP of 3500 or above leads to nanoparticles of unpredictable size with significantly broader, albeit still unimodal, size distributions. Thus this DP appears to represent the realistic upper limit for this PISA formulation.

Representative TEM images for selected PSMA<sub>54</sub>-PBzMA<sub>x</sub> dispersions are shown in Figure 2 (see Figure S2 for additional TEM image). As expected, a kinetically trapped spherical morphology is observed in all cases, even when targeting highly asymmetric diblock copolymer compositions. This is because the PSMA<sub>54</sub> steric stabilizer block is sufficiently long to prevent 1D sphere-sphere fusion occurring during the PISA synthesis.<sup>26</sup> Moreover, although relatively few particles are shown in these images, it seems that the particles are reasonably uniform in size. This tentative finding is supported by DLS

**Table 1.** Summary of Monomer Conversion, GPC, and DLS Data for a Series of PSMA<sub>54</sub>–PBzMA<sub>x</sub> Diblock Copolymers Synthesized via RAFT Dispersion Polymerization of Benzyl Methacrylate in Mineral Oil at 90 °C and 20% w/w Solids (Relevant Data Recorded for the Precursor PSMA<sub>54</sub> Macro-CTA ( $x = 0$ ) Are Shown for Reference)

target PBzMA DP ( $x$ )	<sup>1</sup> H NMR	THF GPC			DLS
	% BzMA	$M_n$ (kg mol <sup>-1</sup> )	$M_w$ (kg mol <sup>-1</sup> )	$M_w/M_n$	$D_h$ (nm)
0		12.7	14.6	1.15	
50	94	17.0	19.3	1.14	24 ± 8
70	97	18.6	21.0	1.14	28 ± 7
90	97	20.2	23.5	1.16	30 ± 7
100	97	21.6	25.1	1.16	32 ± 6
200	98	32.2	39.6	1.23	46 ± 14
400	98	49.8	75.8	1.52	92 ± 16
600	96	62.2	110.0	1.77	147 ± 25
800	96	75.0	175.0	2.33	175 ± 30
1000	97	94.7	236.9	2.50	194 ± 27
1500	99	111.4	346.8	3.11	320 ± 32
2000	99	118.5	357.7	3.02	301 ± 43
2500	98	148.4	438.0	2.95	439 ± 62
3000	98	131.8	424.8	3.22	458 ± 112
3500	98	129.7	442.6	3.41	459 ± 92
4000	98	138.3	457.3	3.31	641 ± 321
4500	98	143.4	474.6	3.31	581 ± 302
5000	97	137.0	476.6	3.48	1108 ± 844

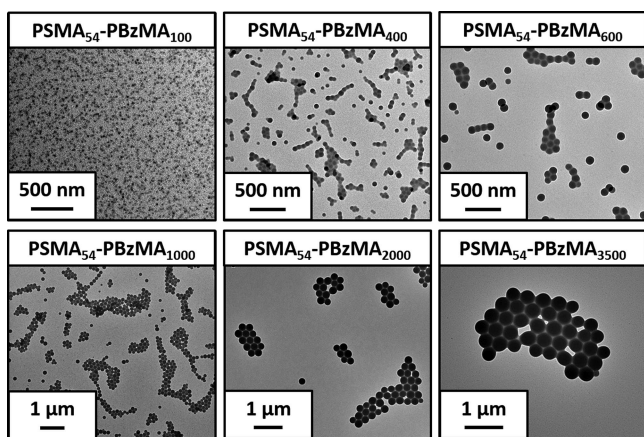


**Figure 2.** Representative transmission electron micrographs recorded for 0.10% w/w dispersions of selected PSMA<sub>54</sub>–PBzMA<sub>x</sub> nanoparticles (see Table 1 for further details).

studies, which indicate that narrow size distributions are obtained for a series of PSMA<sub>54</sub>–PBzMA<sub>x</sub> particles over a wide range of  $x$  values (see Table 1 and Figure 3).

The relationship between the DP of the core-forming PBzMA block ( $x$ ) and the hydrodynamic diameter,  $D_h$ , is shown in Figure 3. In principle, the power-law relationship represented by the linear fit to the data displayed in this double logarithmic plot enables the final particle size to be predicted for a given target PBzMA DP—provided that full BzMA conversion can be achieved for that specific PISA formulation. It is noteworthy that this linear correlation remains valid over a remarkably wide size range, from approximately 24 nm up to 439 nm diameter (where  $x = 50$ –2500). These are among the

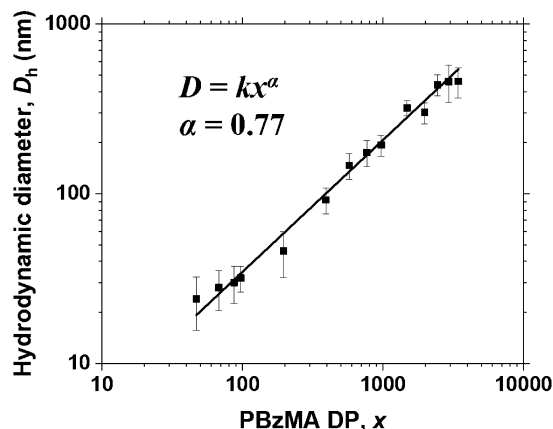


**Figure 3.** Hydrodynamic diameter ( $D_h$ ) vs PBzMA DP ( $x$ ) for a series of PSMA<sub>54</sub>–PBzMA<sub>x</sub> diblock copolymer spheres ( $x = 50$ –3500) prepared via RAFT dispersion polymerization of BzMA in mineral oil at 90 °C and 20% w/w. Error bars represent the standard deviation in  $D_h$  as calculated from the DLS polydispersity index.

largest well-defined spheres with reasonably narrow size distributions (standard deviation  $\leq 20\%$ ) produced by any RAFT-mediated PISA formulation.<sup>26,50–52</sup> The  $\alpha$  exponent calculated for these data (where  $D_h = kx^\alpha$ ) is 0.77, which suggests that the PBzMA chains adopt a relatively stretched (rather than unperturbed) conformation.<sup>53,54</sup> [N.B. For this series of PSMA<sub>54</sub>–PBzMA<sub>x</sub> spheres,  $k = 0.91$ .] In this context, it is perhaps worth mentioning that Tan and co-workers have recently reported that relatively large spheres can be prepared via photoinitiated dispersion polymerization of methyl methacrylate in a 40:60 w/w ethanol/water mixture.<sup>55</sup> In this prior study, such syntheses were conducted in the presence of a binary mixture of RAFT agents, and good size control was achieved despite the rather poor pseudoliving character indicated by GPC analysis.

The robust nature of these PISA formulations is also worth emphasizing. The same PSMA<sub>54</sub> precursor was used by two of the coauthors of this manuscript to target PSMA<sub>54</sub>–PBzMA<sub>x</sub> nanoparticles under the same conditions at 20% w/w solids. For each target PBzMA DP ( $x$ ), hydrodynamic diameters obtained by DLS were almost identical: 301 ± 43 nm vs 302 ± 60 nm ( $x = 2000$ ) and 459 ± 92 nm vs 441 ± 99 nm ( $x = 3500$ ). These experiments indicate predictable mean diameters and reasonably good reproducibility for such PISA syntheses.

Analytical centrifugation can be a powerful technique for the particle size analysis of colloidal dispersions and emulsions.<sup>56–62</sup> Fractionation of the particles occurs prior to their detection, which leads to significantly higher resolution than that achieved for DLS. However, an important input parameter for analytical centrifugation is the particle density: uncertainty in this parameter can lead to large sizing errors. This is a well-known problem in the case of sterically stabilized particles when the steric stabilizer layer is relatively thick compared to the core particle diameter.<sup>63</sup> Analytical centrifugal studies of selected PSMA<sub>54</sub>–PBzMA<sub>x</sub> spheres were undertaken at 1.0% w/w to minimize hindered sedimentation, which leads to sizing errors for concentrated dispersions.<sup>64,65</sup> The resulting particle size distributions are shown for three dispersions in Figure 4, where  $x = 1000$ , 2000, and 3500. For PSMA<sub>54</sub>–PBzMA<sub>2000</sub> and PSMA<sub>54</sub>–PBzMA<sub>3500</sub>, the effective particle density is sufficiently close to the density of the PBzMA nanoparticle cores ( $\rho_{\text{PBzMA}} = 1.15 \text{ g cm}^{-3}$ ) that there is no

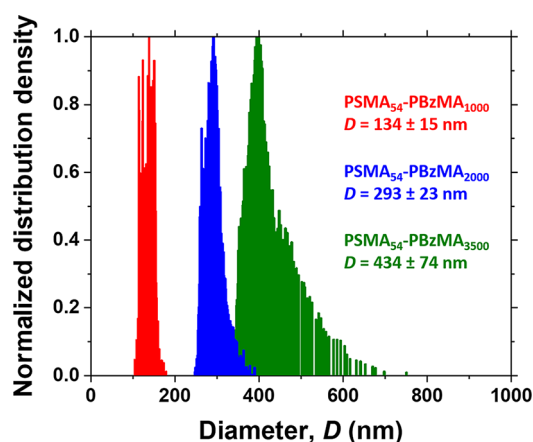


**Figure 4.** Volume-average particle size distributions obtained via analytical centrifugation at 20 °C for PSMA<sub>54</sub>-PBzMA<sub>1000</sub> (red data), PSMA<sub>54</sub>-PBzMA<sub>2000</sub> (blue data), and PSMA<sub>54</sub>-PBzMA<sub>3500</sub> (green data).

appreciable sizing error. Thus the volume-average diameters are slightly lower than the corresponding intensity-average diameters reported by DLS (see Table 1), as expected. However, this is not the case for PSMA<sub>54</sub>-PBzMA<sub>1000</sub>; hence, analytical centrifugation (135 ± 15 nm) significantly under-sizes compared to DLS (194 ± 27 nm) owing to an inaccurate (i.e., too high) effective particle density.

Finally, the long-term stability of 20% w/w copolymer dispersions after storage at ambient temperature for approximately two years was assessed by DLS (after dilution to produce 0.10% w/w dispersions). PSMA<sub>54</sub>-PBzMA<sub>x</sub> spheres for which  $x \leq 1000$  (i.e., below 200 nm diameter) remained colloidally stable over this time period, with comparable intensity-average hydrodynamic diameters (and corresponding standard deviations) being obtained compared to the freshly synthesized nanoparticles (see Table S1). However, significant irreversible aggregation was observed for PSMA<sub>54</sub>-PBzMA<sub>x</sub> dispersions when targeting higher  $x$  values. The reason for this unexpected loss in colloidal stability is not known and warrants further study.

## CONCLUSIONS

The upper size limit has been established for the preparation of PSMA<sub>54</sub>-PBzMA<sub>x</sub> nanoparticles via PISA at 20% w/w solids. Well-defined spheres (standard deviations  $\leq 20\%$ ) can be obtained with mean hydrodynamic diameters of up to 459 nm when targeting a core-forming PBzMA DP of 3500. In principle, the power-law relationship between hydrodynamic diameter and PBzMA DP enables convenient targeting of any desired particle size up to this limiting value. Gradual loss in RAFT control over the BzMA polymerization is observed, with GPC analysis indicating  $M_w/M_n$  values increasing from 1.14 up to 3.41. Nevertheless, broad MWDs do not prevent the formation of well-defined sterically stabilized nanoparticles with reasonably narrow size distributions. However, targeting PBzMA DPs above 3500 leads to the formation of particles with relatively broad size distributions and unpredictable mean diameters. Large (>300 nm diameter) PSMA<sub>54</sub>-PBzMA<sub>x</sub> spheres were identified as suitable nanoparticles for analytical centrifugation studies, because in this size regime the overall nanoparticle density is approximately the same as that for the core-forming PBzMA block.

## ASSOCIATED CONTENT

### Supporting Information

The Supporting Information is available free of charge at <https://pubs.acs.org/doi/10.1021/acs.langmuir.0c00211>.

Additional TEM image and DLS colloidal stability study (PDF)

## AUTHOR INFORMATION

### Corresponding Authors

**Matthew J. Derry** – Dainton Building, Department of Chemistry, University of Sheffield, Brook Hill, Sheffield, South Yorkshire S3 7HF, United Kingdom; [orcid.org/0000-0001-5010-6725](https://orcid.org/0000-0001-5010-6725); Email: [m.derry@aston.ac.uk](mailto:m.derry@aston.ac.uk)

**Steven P. Armes** – Dainton Building, Department of Chemistry, University of Sheffield, Brook Hill, Sheffield, South Yorkshire S3 7HF, United Kingdom; [orcid.org/0000-0002-8289-6351](https://orcid.org/0000-0002-8289-6351); Email: [s.p.ames@sheffield.ac.uk](mailto:s.p.ames@sheffield.ac.uk)

### Authors

**Bryony R. Parker** – Dainton Building, Department of Chemistry, University of Sheffield, Brook Hill, Sheffield, South Yorkshire S3 7HF, United Kingdom

**Yin Ning** – Dainton Building, Department of Chemistry, University of Sheffield, Brook Hill, Sheffield, South Yorkshire S3 7HF, United Kingdom; [orcid.org/0000-0003-1808-3513](https://orcid.org/0000-0003-1808-3513)

Complete contact information is available at:

<https://pubs.acs.org/10.1021/acs.langmuir.0c00211>

### Notes

The authors declare no competing financial interest.

## ACKNOWLEDGMENTS

S.P.A. thanks EPSRC for a four-year *Established Career* Particle Technology Fellowship (EP/J003009/1). M.J.D. and S.P.A. thank the Leverhulme Trust for a postdoctoral fellowship (RPG-2016-330). Dr. S. Tzokov at The University of Sheffield Biomedical Science Electron Microscopy Suite is thanked for TEM assistance.

## REFERENCES

- (1) Charleux, B.; Delaittre, G.; Rieger, J.; D'Agosto, F. Polymerization-induced self-assembly: From soluble macromolecules to block copolymer nano-objects in one step. *Macromolecules* **2012**, *45* (17), 6753–6765.
- (2) Monteiro, M. J.; Cunningham, M. F. Polymer nanoparticles via living radical polymerization in aqueous dispersions: Design and applications. *Macromolecules* **2012**, *45* (12), 4939–4957.
- (3) Sun, J.-T.; Hong, C.-Y.; Pan, C.-Y. Formation of the block copolymer aggregates via polymerization-induced self-assembly and reorganization. *Soft Matter* **2012**, *8* (30), 7753–7767.
- (4) Derry, M. J.; Fielding, L. A.; Armes, S. P. Polymerization-induced self-assembly of block copolymer nanoparticles via RAFT non-aqueous dispersion polymerization. *Prog. Polym. Sci.* **2016**, *52*, 1–18.
- (5) D'Agosto, F.; Rieger, J.; Lansalot, M. RAFT-mediated polymerization-induced self-assembly. *Angew. Chem.* **2019**, in press. DOI: [10.1002/ange.201911758](https://doi.org/10.1002/ange.201911758).
- (6) Rieger, J.; Stoffelbach, F.; Bui, C.; Alaimo, D.; Jerome, C.; Charleux, B. Amphiphilic poly(ethylene oxide) macromolecular RAFT agent as a stabilizer and control agent in ab initio batch emulsion polymerization. *Macromolecules* **2008**, *41* (12), 4065–4068.
- (7) Rieger, J.; Grazon, C.; Charleux, B.; Alaimo, D.; Jérôme, C. Pegylated thermally responsive block copolymer micelles and nanogels via in situ RAFT aqueous dispersion polymerization. *J. Polym. Sci., Part A: Polym. Chem.* **2009**, *47* (9), 2373–2390.

- (8) Boisse, S.; Rieger, J.; Belal, K.; Di-Cicco, A.; Beaunier, P.; Li, M.-H.; Charleux, B. Amphiphilic block copolymer nano-fibers via RAFT-mediated polymerization in aqueous dispersed system. *Chem. Commun.* **2010**, 46 (11), 1950–1952.
- (9) Zhang, X.; Boisse, S.; Zhang, W.; Beaunier, P.; D'Agosto, F.; Rieger, J.; Charleux, B. Well-defined amphiphilic block copolymers and nano-objects formed in situ via RAFT-mediated aqueous emulsion polymerization. *Macromolecules* **2011**, 44 (11), 4149–4158.
- (10) Chaduc, I.; Zhang, W. J.; Rieger, J.; Lansalot, M.; D'Agosto, F.; Charleux, B. Amphiphilic block copolymers from a direct and one-pot RAFT synthesis in water. *Macromol. Rapid Commun.* **2011**, 32 (16), 1270–1276.
- (11) Blanazs, A.; Madsen, J.; Battaglia, G.; Ryan, A. J.; Armes, S. P. Mechanistic insights for block copolymer morphologies: How do worms form vesicles? *J. Am. Chem. Soc.* **2011**, 133 (41), 16581–16587.
- (12) Cai, W.; Wan, W.; Hong, C.; Huang, C.; Pan, C. Morphology transitions in RAFT polymerization. *Soft Matter* **2010**, 6 (21), 5554–5561.
- (13) Wan, W. M.; Pan, C. Y. Formation of polymeric yolk/shell nanomaterial by polymerization-induced self-assembly and reorganization. *Macromolecules* **2010**, 43 (6), 2672–2675.
- (14) Wan, W.-M.; Pan, C.-Y. One-pot synthesis of polymeric nanomaterials via RAFT dispersion polymerization induced self-assembly and re-organization. *Polym. Chem.* **2010**, 1 (9), 1475–1484.
- (15) He, W.-D.; Sun, X.-L.; Wan, W.-M.; Pan, C.-Y. Multiple morphologies of PAA-b-PSt assemblies throughout RAFT dispersion polymerization of styrene with PAA macro-CTA. *Macromolecules* **2011**, 44 (9), 3358–3365.
- (16) Pei, Y.; Lowe, A. B. Polymerization-induced self-assembly: Ethanolic RAFT dispersion polymerization of 2-phenylethyl methacrylate. *Polym. Chem.* **2014**, 5 (7), 2342–2351.
- (17) Pei, Y. W.; Noy, J. M.; Roth, P. J.; Lowe, A. B. Thiol-reactive Passerini-methacrylates and polymorphic surface functional soft matter nanoparticles via ethanolic RAFT dispersion polymerization and post-synthesis modification. *Polym. Chem.* **2015**, 6 (11), 1928–1931.
- (18) Zhang, W.-J.; Hong, C.-Y.; Pan, C.-Y. Formation of hexagonally packed hollow hoops and morphology transition in RAFT ethanolic dispersion polymerization. *Macromol. Rapid Commun.* **2015**, 36 (15), 1428–1436.
- (19) Zhao, W.; Gody, G.; Dong, S. M.; Zetterlund, P. B.; Perrier, S. Optimization of the RAFT polymerization conditions for the in situ formation of nano-objects via dispersion polymerization in alcoholic medium. *Polym. Chem.* **2014**, 5 (24), 6990–7003.
- (20) Houillot, L.; Bui, C.; Save, M.; Charleux, B.; Farcet, C.; Moire, C.; Raust, J.-A.; Rodriguez, I. Synthesis of well-defined polyacrylate particle dispersions in organic medium using simultaneous RAFT polymerization and self-assembly of block copolymers. A strong influence of the selected thiocarbonylthio chain transfer agent. *Macromolecules* **2007**, 40 (18), 6500–6509.
- (21) Houillot, L.; Bui, C.; Farcet, C.; Moire, C.; Raust, J.-A.; Pasch, H.; Save, M.; Charleux, B. Dispersion polymerization of methyl acrylate in nonpolar solvent stabilized by block copolymers formed in situ via the RAFT process. *ACS Appl. Mater. Interfaces* **2010**, 2 (2), 434–442.
- (22) Fielding, L. A.; Lane, J. A.; Derry, M. J.; Mykhaylyk, O. O.; Armes, S. P. Thermo-responsive diblock copolymer worm gels in non-polar solvents. *J. Am. Chem. Soc.* **2014**, 136 (15), 5790–5798.
- (23) Pei, Y.; Thurairajah, L.; Sugita, O. R.; Lowe, A. B. RAFT dispersion polymerization in nonpolar media: Polymerization of 3-phenylpropyl methacrylate in n-tetradecane with poly(stearyl methacrylate) homopolymers as macro chain transfer agents. *Macromolecules* **2015**, 48 (1), 236–244.
- (24) Pei, Y.; Noy, J.-M.; Roth, P. J.; Lowe, A. B. Soft matter nanoparticles with reactive coronal pentafluorophenyl methacrylate residues via non-polar RAFT dispersion polymerization and polymerization-induced self-assembly. *J. Polym. Sci., Part A: Polym. Chem.* **2015**, 53, 2326–2335.
- (25) Pei, Y.; Sugita, O. R.; Thurairajah, L.; Lowe, A. B. Synthesis of poly(stearyl methacrylate-b-3-phenylpropyl methacrylate) nanoparticles in n-octane and associated thermoreversible polymorphism. *RSC Adv.* **2015**, 5 (23), 17636–17646.
- (26) Derry, M. J.; Fielding, L. A.; Warren, N. J.; Mable, C. J.; Smith, A. J.; Mykhaylyk, O. O.; Armes, S. P. In situ small-angle X-ray scattering studies of sterically-stabilized diblock copolymer nanoparticles formed during polymerization-induced self-assembly in non-polar media. *Chemical Science* **2016**, 7, 5078–5090.
- (27) Derry, M. J.; Mykhaylyk, O. O.; Armes, S. P. A vesicle-to-worm transition provides a new high-temperature oil thickening mechanism. *Angew. Chem., Int. Ed.* **2017**, 56 (7), 1746–1750.
- (28) Smith, G. N.; Derry, M. J.; Hallett, J. E.; Lovett, J. R.; Mykhaylyk, O. O.; Neal, T. J.; Prevost, S.; Armes, S. P. Refractive index matched, nearly hard polymer colloids. *Proc. R. Soc. London, Ser. A* **2019**, 475 (2226), 20180763.
- (29) Fielding, L. A.; Derry, M. J.; Ladmiral, V.; Rosselgong, J.; Rodrigues, A. M.; Ratcliffe, L. P. D.; Sugihara, S.; Armes, S. P. RAFT dispersion polymerization in non-polar solvents: facile production of block copolymer spheres, worms and vesicles in n-alkanes. *Chemical Science* **2013**, 4 (5), 2081–2087.
- (30) Derry, M. J.; Fielding, L. A.; Armes, S. P. Industrially-relevant polymerization-induced self-assembly formulations in non-polar solvents: RAFT dispersion polymerization of benzyl methacrylate. *Polym. Chem.* **2015**, 6 (16), 3054–3062.
- (31) Derry, M. J.; Mykhaylyk, O. O.; Ryan, A. J.; Armes, S. P. Thermoreversible crystallization-driven aggregation of diblock copolymer nanoparticles in mineral oil. *Chemical Science* **2018**, 9 (17), 4071–4082.
- (32) Jenkins, A. D. Molecular architecture through group-transfer polymerization. *Makromol. Chem., Macromol. Symp.* **1992**, 53, 267–273.
- (33) Yamauchi, K.; Hasegawa, H.; Hashimoto, T.; Tanaka, H.; Motokawa, R.; Koizumi, S. Direct observation of polymerization-reaction-induced molecular self-assembling process: In-situ and real-time SANS measurements during living anionic polymerization of polyisoprene-block-polystyrene. *Macromolecules* **2006**, 39 (13), 4531–4539.
- (34) Chiefari, J.; Chong, Y. K.; Ercole, F.; Krstina, J.; Jeffery, J.; Le, T. P. T.; Mayadunne, R. T. A.; Meijs, G. F.; Moad, C. L.; Moad, G.; Rizzardo, E.; Thang, S. H. Living free-radical polymerization by reversible addition-fragmentation chain transfer: The RAFT process. *Macromolecules* **1998**, 31 (16), 5559–5562.
- (35) Moad, G.; Rizzardo, E.; Thang, S. H. Radical addition-fragmentation chemistry in polymer synthesis. *Polymer* **2008**, 49 (5), 1079–1131.
- (36) Perrier, S. 50th Anniversary Perspective: RAFT Polymerization—A User Guide. *Macromolecules* **2017**, 50 (19), 7433–7447.
- (37) Destarac, M. Industrial development of reversible-deactivation radical polymerization: is the induction period over? *Polym. Chem.* **2018**, 9 (40), 4947–4967.
- (38) Barner-Kowollik, C.; Perrier, S. The future of reversible addition fragmentation chain transfer polymerization. *J. Polym. Sci., Part A: Polym. Chem.* **2008**, 46 (17), 5715–5723.
- (39) Ratcliffe, L. P. D.; McKenzie, B. E.; Le Bouëdec, G. M. D.; Williams, C. N.; Brown, S. L.; Armes, S. P. Polymerization-induced self-assembly of all-acrylic diblock copolymers via RAFT dispersion polymerization in alkanes. *Macromolecules* **2015**, 48 (23), 8594–8607.
- (40) Smith, G. N.; Alexander, S.; Brown, P.; Gillespie, D. A. J.; Grillo, I.; Heenan, R. K.; James, C.; Kemp, R.; Rogers, S. E.; Eastoe, J. Interaction between surfactants and colloidal latexes in nonpolar solvents studied using contrast-variation small-angle neutron scattering. *Langmuir* **2014**, 30 (12), 3422–3431.
- (41) Smith, G. N.; Grillo, I.; Rogers, S. E.; Eastoe, J. Surfactants with colloids: Adsorption or absorption? *J. Colloid Interface Sci.* **2015**, 449, 205–214.
- (42) Richez, A. P.; Yow, H. N.; Biggs, S.; Cayre, O. J. Dispersion polymerization in non-polar solvent: Evolution toward emerging applications. *Prog. Polym. Sci.* **2013**, 38 (6), 897–931.

- (43) Richez, A. P.; Farrand, L.; Goulding, M.; Wilson, J. H.; Lawson, S.; Biggs, S.; Cayre, O. J. Poly(dimethylsiloxane)-stabilized polymer particles from radical dispersion polymerization in nonpolar solvent: Influence of stabilizer properties and monomer type. *Langmuir* **2014**, *30* (5), 1220–1228.
- (44) Belsey, K. E.; Topping, C.; Farrand, L. D.; Holder, S. J. Inhibiting the thermal gelation of copolymer stabilized nonaqueous dispersions and the synthesis of full color PMMA particles. *Langmuir* **2016**, *32* (11), 2556–2566.
- (45) Derry, M. J.; Smith, T.; O'Hora, P. S.; Armes, S. P. Block copolymer nanoparticles prepared via polymerization-induced self-assembly provide excellent boundary lubrication performance for next-generation ultralow-viscosity automotive engine oils. *ACS Appl. Mater. Interfaces* **2019**, *11*, 33364.
- (46) Rymaruk, M. J.; Thompson, K. L.; Derry, M. J.; Warren, N. J.; Ratcliffe, L. P. D.; Williams, C. N.; Brown, S. L.; Armes, S. P. Bespoke contrast-matched diblock copolymer nanoparticles enable the rational design of highly transparent Pickering double emulsions. *Nanoscale* **2016**, *8* (30), 14497–14506.
- (47) Trent, J. S. Ruthenium tetraoxide staining of polymers - new preparative methods for electron-microscopy. *Macromolecules* **1984**, *17* (12), 2930–2931.
- (48) Donovan, M. S.; Lowe, A. B.; Sumerlin, B. S.; McCormick, C. L. Raft polymerization of N, N-dimethylacrylamide utilizing novel chain transfer agents tailored for high reinitiation efficiency and structural control. *Macromolecules* **2002**, *35* (10), 4123–4132.
- (49) Moad, G.; Chiefari, J.; Mayadunne, R. T. A.; Moad, C. L.; Postma, A.; Rizzardo, E.; Thang, S. H. Initiating free radical polymerization. *Macromol. Symp.* **2002**, *182* (1), 65–80.
- (50) Cunningham, V. J.; Alswieleh, A. M.; Thompson, K. L.; Williams, M.; Leggett, G. J.; Armes, S. P.; Musa, O. M. Poly(glycerol monomethacrylate)-poly(benzyl methacrylate) diblock copolymer nanoparticles via RAFT emulsion polymerization: Synthesis, characterization, and interfacial activity. *Macromolecules* **2014**, *47* (16), 5613–5623.
- (51) Akpınar, B.; Fielding, L. A.; Cunningham, V. J.; Ning, Y.; Mykhaylyk, O. O.; Fowler, P. W.; Armes, S. P. Determining the effective density and stabilizer layer thickness of sterically stabilized nanoparticles. *Macromolecules* **2016**, *49* (14), 5160–5171.
- (52) Truong, N. P.; Dussert, M. V.; Whittaker, M. R.; Quinn, J. F.; Davis, T. P. Rapid synthesis of ultrahigh molecular weight and low polydispersity polystyrene diblock copolymers by RAFT-mediated emulsion polymerization. *Polym. Chem.* **2015**, *6* (20), 3865–3874.
- (53) Leibler, L. Theory of microphase separation in block copolymers. *Macromolecules* **1980**, *13* (6), 1602–1617.
- (54) Förster, S.; Zisenis, M.; Wenz, E.; Antonietti, M. Micellization of strongly segregated block copolymers. *J. Chem. Phys.* **1996**, *104* (24), 9956–9970.
- (55) Yu, L.; Dai, X.; Zhang, Y.; Zeng, Z.; Zhang, L.; Tan, J. Better RAFT control is better? Insights into the preparation of monodisperse surface-functional polymeric microspheres by photoinitiated RAFT dispersion polymerization. *Macromolecules* **2019**, *52* (19), 7267–7277.
- (56) Lerche, D. Dispersion stability and particle characterization by sedimentation kinetics in a centrifugal field. *J. Dispersion Sci. Technol.* **2002**, *23* (5), 699–709.
- (57) Detloff, T.; Sobisch, T.; Lerche, D. Particle size distribution by space or time dependent extinction profiles obtained by analytical centrifugation (concentrated systems). *Powder Technol.* **2007**, *174* (1–2), 50–55.
- (58) Petzold, G.; Goltzsche, C.; Mende, M.; Schwarz, S.; Jaeger, W. Monitoring the stability of nanosized silica dispersions in presence of polycations by a novel centrifugal sedimentation method. *J. Appl. Polym. Sci.* **2009**, *114* (2), 696–704.
- (59) Yow, H. N.; Biggs, S. Probing the stability of sterically stabilized polystyrene particles by centrifugal sedimentation. *Soft Matter* **2013**, *9* (42), 10031–10041.
- (60) Growney, D. J.; Mykhaylyk, O. O.; Middlemiss, L.; Fielding, L. A.; Derry, M. J.; Aragrag, N.; Lamb, G. D.; Armes, S. P. Is carbon black a suitable model colloidal substrate for diesel soot? *Langmuir* **2015**, *31* (38), 10358–10369.
- (61) Thompson, K. L.; Derry, M. J.; Hatton, F. L.; Armes, S. P. Long-term stability of n-alkane-in-water Pickering nanoemulsions: Effect of aqueous solubility of droplet phase on Ostwald ripening. *Langmuir* **2018**, *34* (31), 9289–9297.
- (62) Walter, J.; Thajudeen, T.; Süß, S.; Segets, D.; Peukert, W. New possibilities of accurate particle characterisation by applying direct boundary models to analytical centrifugation. *Nanoscale* **2015**, *7* (15), 6574–6587.
- (63) Growney, D. J.; Fowler, P. W.; Mykhaylyk, O. O.; Fielding, L. A.; Derry, M. J.; Aragrag, N.; Lamb, G. D.; Armes, S. P. Determination of effective particle density for sterically stabilized carbon black particles: Effect of diblock copolymer stabilizer composition. *Langmuir* **2015**, *31* (32), 8764–8773.
- (64) He, P.; Mejia, A. F.; Cheng, Z.; Sun, D.; Sue, H.-J.; Dinair, D. S.; Marquez, M. Hindrance function for sedimentation and creaming of colloidal disks. *Phys. Rev. E* **2010**, *81* (2), 026310.
- (65) Lerche, D. Comprehensive characterization of nano- and microparticles by in-situ visualization of particle movement using advanced sedimentation techniques. *KONA Powder and Particle Journal* **2019**, *36*, 156–186.